



Properties of 249 δ Scuti Variable Star Candidates Observed During the NASA K2 Mission

Joyce Ann Guzik^{1*}, Jorge A. Garcia² and Jason Jackiewicz²

¹ Theoretical Design Division and Center for Theoretical Astrophysics, Los Alamos National Laboratory, Los Alamos, NM, United States, ² Department of Astronomy, New Mexico State University, Las Cruces, NM, United States

OPEN ACCESS

Edited by:

Jadwiga Daszynska-Daszkiewicz,
University of Wrocław, Poland

Reviewed by:

Andrzej S. Baran,
Pedagogical University of Kraków,
Poland
Margit Paparo,
Konkoly Observatory (MTA), Hungary

*Correspondence:

Joyce Ann Guzik
joy@lanl.gov

Specialty section:

This article was submitted to
Stellar and Solar Physics,
a section of the journal
*Frontiers in Astronomy and Space
Sciences*

Received: 16 January 2019

Accepted: 09 May 2019

Published: 31 May 2019

Citation:

Guzik JA, Garcia JA and Jackiewicz J (2019) Properties of 249 δ Scuti Variable Star Candidates Observed During the NASA K2 Mission. *Front. Astron. Space Sci.* 6:40. doi: 10.3389/fspas.2019.00040

In the second phase of the NASA *Kepler* mission (K2), the *Kepler* spacecraft observed fields along the ecliptic plane for about 80 days each to search for planetary transits and monitor stellar variability. We analyzed the light curves of thousands of main-sequence stars observed as part of the *Kepler* Guest Observer program. Here we summarize the statistics of discovery and properties of the pulsation amplitude spectra for 249 δ Scuti variable stars or candidates observed during K2 Campaigns 4 through 17. δ Sct variables are core or shell hydrogen-burning stars about twice as massive as the Sun, pulsating in many simultaneous radial and non-radial modes, with periods of about 2 h. The growing collection of long time-series high signal-to-noise photometric data from space missions such as *Kepler*, combined with constraints from ground and space-based data, will be useful to constrain the interior structure of these types of variables. We hope that this list of δ Sct candidates observed by *Kepler* will be useful as a starting point for identifying promising targets for asteroseismic investigations.

Keywords: NASA *Kepler* mission, stars: δ Sct, stars: γ Dor, photometry, stars: variable, stars: main-sequence

1. INTRODUCTION

The NASA *Kepler* mission was launched March 6, 2009, with a primary objective to use high-precision long time-series CCD photometry to search for exoplanets via planetary transits, and a secondary mission to study stellar variability and characterize exoplanet host stars (Borucki et al., 2010; Gilliland et al., 2010; Lundkvist et al., 2018). Stellar pulsations can be used to infer the interior structure of stars, and to determine their masses, radii, and ages, some of the goals of the field of asteroseismology (Aerts et al., 2010). The K2 mission was devised in 2013 (Howell et al., 2014), after failure of the second of four reaction wheels that were used to point the spacecraft cameras continuously toward the same field of view in the Cygnus-Lyra region to monitor stars for planetary transits. K2 relied on solar radiation pressure to assist spacecraft orientation, and observed 19 new fields along the ecliptic plane for up to 80 days each. The spacecraft eventually exhausted its fuel and was retired on November 15, 2018¹.

We report on analyses of light curves from the K2 mission from Campaigns 4 through 17 obtained as part of the *Kepler* K2 Guest Observer program². We focus here on searching for δ Sct variable star candidates. The δ Sct variables are main-sequence stars (core or shell hydrogen-burning), with effective temperature (T_{eff}) about 7,000 K and masses of about $2 M_{\odot}$ that

¹<https://exoplanets.nasa.gov/news/1534/goodnight-kepler-final-commands-for-space-telescope>

²<https://keplerscience.arc.nasa.gov/k2-approved-programs.html>

TABLE 1 | K2 Guest Observer survey results, with number of stars observed, minimum, and maximum *Kepler* magnitudes of stars observed in campaign, and number of identified δ Sct candidates.

Campaign	# Stars Observed	min Kp mag (brightest)	max Kp mag (faintest)	# δ Sct Candidates	Comment
C4	894	2.99	16.6	9	Pleiades/Hyades
C5	1268	6.20	19.8	12	M67/Beehive
C6	996	6.04	15.0	4	North Galactic Cap
C7	506	7.37	16.5	23	R147, near Gal. Center
C8	3370	6.04	16.0	5	
C10	2500	6.06	15.8	5	North Galactic Cap
C11	2814	6.09	13.2	107	Galactic Center
C12	1859	5.98	15.9	15	
C13	2890	5.12	15.9	69	Hyades
C17	560	6.04	15.0	2	Overlap with C6

pulsate in many simultaneous radial and non-radial modes with periods of about 2 h (Aerts et al., 2010). *Kepler* photometry can detect brightness variations produced by radial and low-degree non-radial acoustic (p-mode) pulsations for which the variations do not average out over the unresolved disk.

Apart from the Sun and sun-like stars, the δ Sct variables are arguably the most promising type of variable for using pulsations to infer interior structure. Similarities to and differences from the Sun can be used test physics input and methods of solar and stellar modeling. For example, the δ Sct stars have convective cores and radiative envelopes, whereas the Sun has a radiative core and convective envelope. The δ Sct p-mode pulsations are driven by the κ effect (opacity valving) mechanism, whereas solar-like oscillations are excited stochastically (Aerts et al., 2010). Most δ Sct variables rotate more rapidly than the Sun. Many interesting phenomena remain to be explained, for example, mode selection, pulsation amplitudes, frequency and mode amplitude variations, peculiar element abundances, and the prevalence of many hybrid stars showing both γ Dor gravity-mode and δ Sct p-mode pulsations, unexpected according to pre-*Kepler* theoretical predictions (see, e.g., Grigahcène et al., 2010; Uytterhoeven et al., 2011; Balona, 2018).

2. DATA AND ANALYSIS METHODS

For our K2 Guest Observer (GO) program proposals, we used the MAST interface to the K2 Ecliptic Plane Input Catalog, EPIC³ Huber et al. (2017), to search for stars within the coordinates of the K2 campaign field of view having either B-V or J-K colors between -0.3 and 1.2 , placing them on or near the main sequence, allowing for uncertainties in color photometry or interstellar reddening. We used the k2fov tool found at the *Kepler* Asteroseismic Science Consortium web site⁴ to retain only targets that fell on active silicon in the *Kepler* field of view, and limited our target lists depending on campaign constraints. The target lists were truncated as necessary by the K2 GO office by removing the faintest targets first (at our request) or the

brightest targets that are most costly in terms of number of pixels required. **Table 1** summarizes the number of light curves observed for each campaign, and the brightest (Kp minimum) and faintest (Kp maximum) *Kepler* magnitude of the sample. For Campaigns 4, 5, and 7, we deliberately targeted open-cluster stars in the Pleiades, Hyades, M67, M44 (also known as the Praesepe or Beehive cluster), and R147, based on catalogs of cluster member candidates. The C13 field also has a small overlap with the C4 field and includes Hyades members. We did not propose K2 GO surveys for C14-C16, but in the future we could analyze light curves in the K2 data archive for these campaigns having the same target selection criteria. The C17 field significantly overlapped that of C6, and we deliberately chose to revisit stars with prior observations to extend the time series of observations. The two δ Sct candidates found in C17 in **Table 1** were also found in C6. We have yet to analyze data from our C18 and C19 proposed observations, also revisiting many stars observed previously in Campaigns 5 and 12.

Here we analyze light curves with long-cadence observations (30 min integrations), although several of the stars were observed also in short cadence (1 min integrations) for our or others' Guest Observer programs. We developed a Python script with a graphical interface⁵ that processed the fits files for raw data available at the MAST K2 archive⁶, and plotted the light curve and amplitude spectrum for each star, displaying also stellar properties in the data file header from the EPIC catalog. Because of the 30 min cadence and associated Nyquist frequency limit of 24.5 cycles/day (c/d), we do not consider frequencies above the Nyquist limit; some modes with frequencies above this limit may appear as 'Nyquist reflection' frequencies between 0 and 24.5 c/d (see, e.g., Murphy et al., 2013).

We then examined by eye each light and amplitude spectrum, and flagged as δ Sct candidates those stars with one or more modes with frequency > 5 c/d and amplitude greater than about $4\times$ the noise level of the adjacent power spectrum. We did not flag as δ Sct candidates those stars

³<https://archive.stsci.edu/k2/epic/search.php>

⁴<https://kasoc.phys.au.dk/tools/k2fov>

⁵<https://github.com/JorgeAGR/stat-var-stars>

⁶https://archive.stsci.edu/k2/data_search/search.php

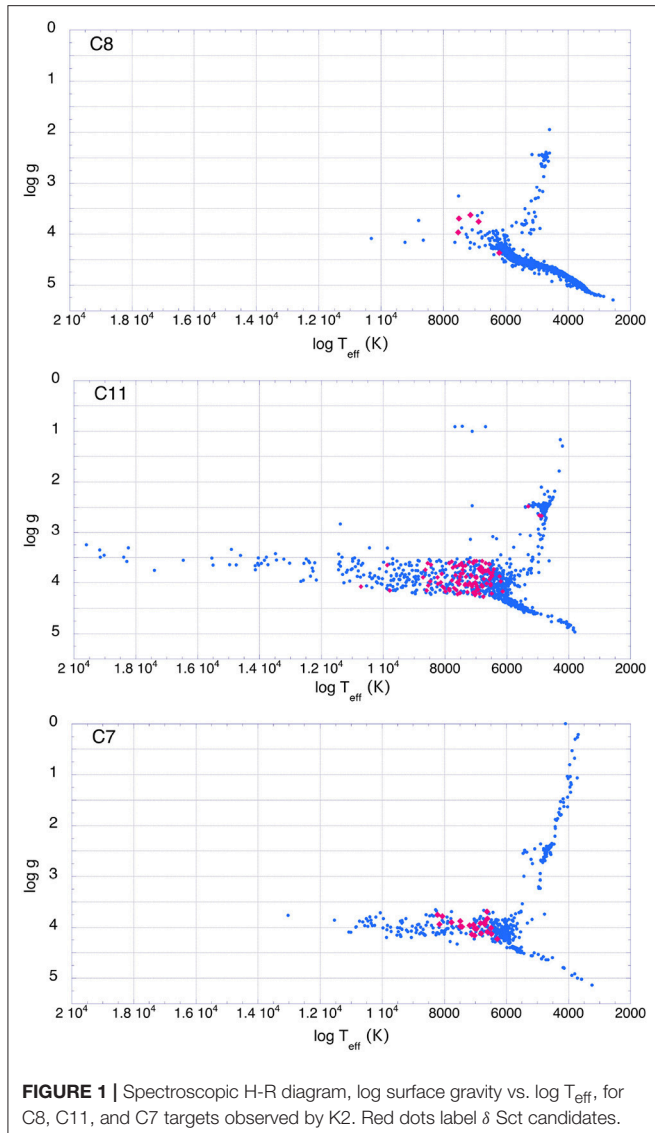


FIGURE 1 | Spectroscopic H-R diagram, \log surface gravity vs. $\log T_{\text{eff}}$, for C8, C11, and C7 targets observed by K2. Red dots label δ Sct candidates.

for which the amplitude spectrum shows only frequencies that are multiples of the spacecraft roll correction period of ~ 6 h (4.075 c/d) that are highlighted in the amplitude spectra plots. Some candidates were discarded, such as those having only low signal-to-noise frequencies > 5 c/d; there could therefore be many more δ Sct stars among the observed sample. It would also be useful to identify those stars with T_{eff} placing them within the δ Sct instability region, but that show no apparent pulsation frequencies. We did not attempt to identify γ Dor candidates because these would be much more numerous, being less massive, and because of the high potential of ambiguities between intrinsic pulsation frequencies and a rotational period or variation from starspots/magnetic activity, a binary orbital period, instrumental artifacts, or Nyquist reflections of higher frequencies. Overall, 251 δ Sct candidates were flagged, two of which in C17 also were found in C6 (see Table 1). The percentage of δ

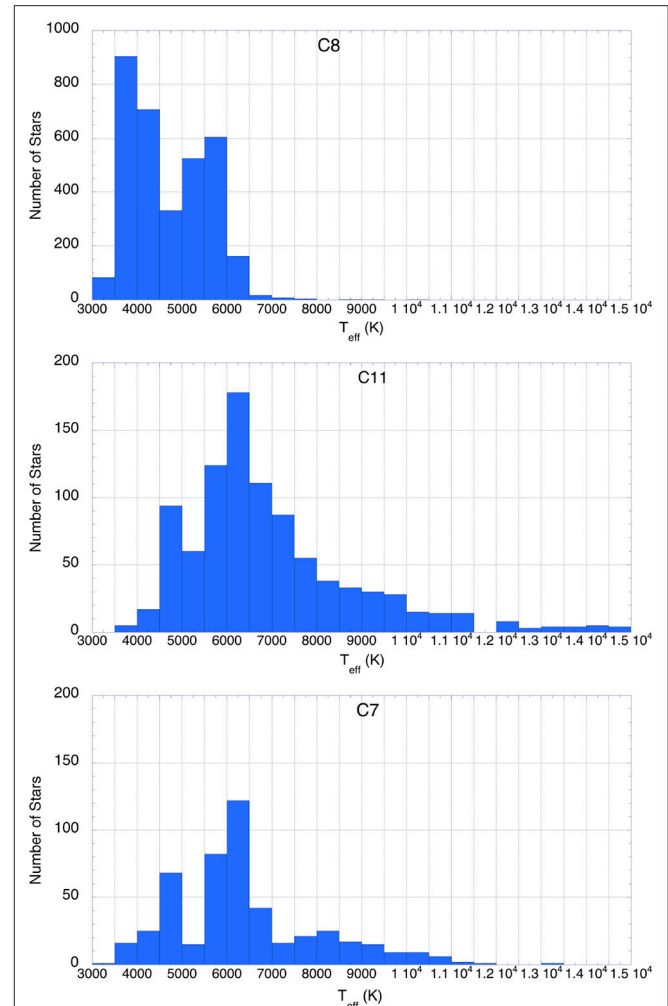
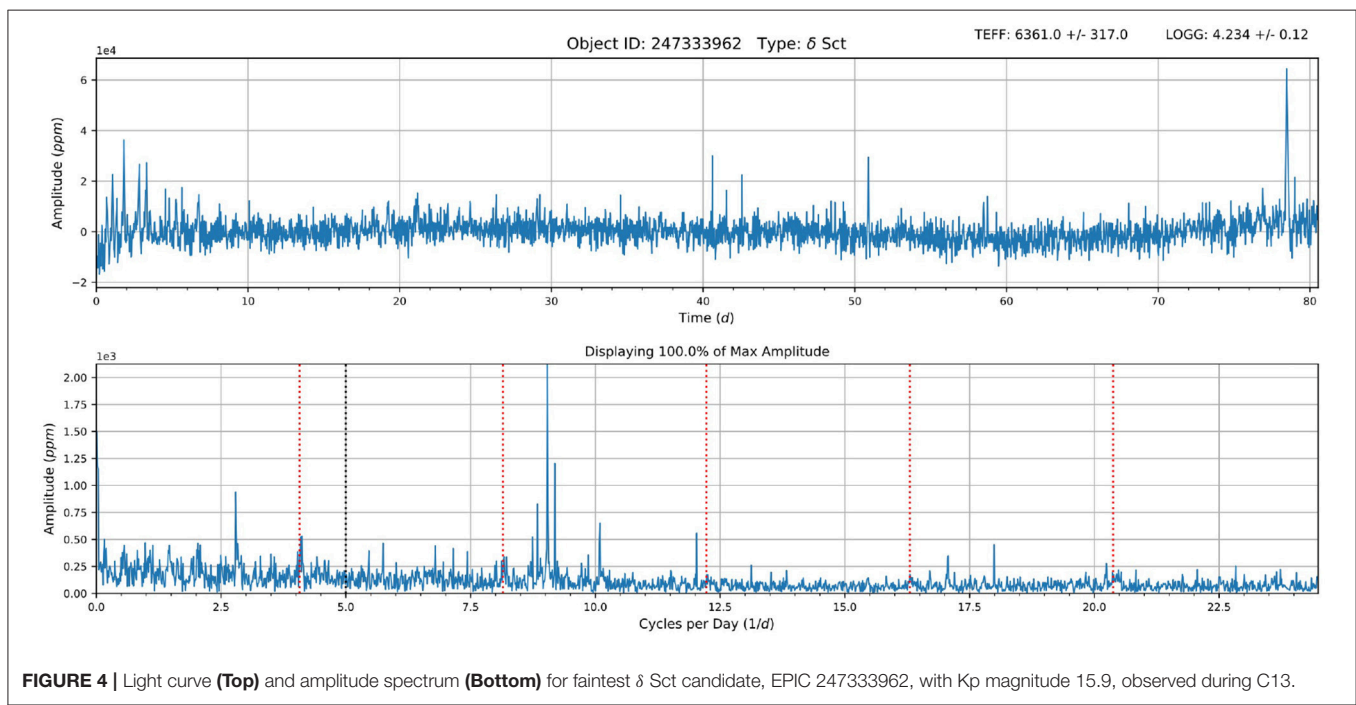
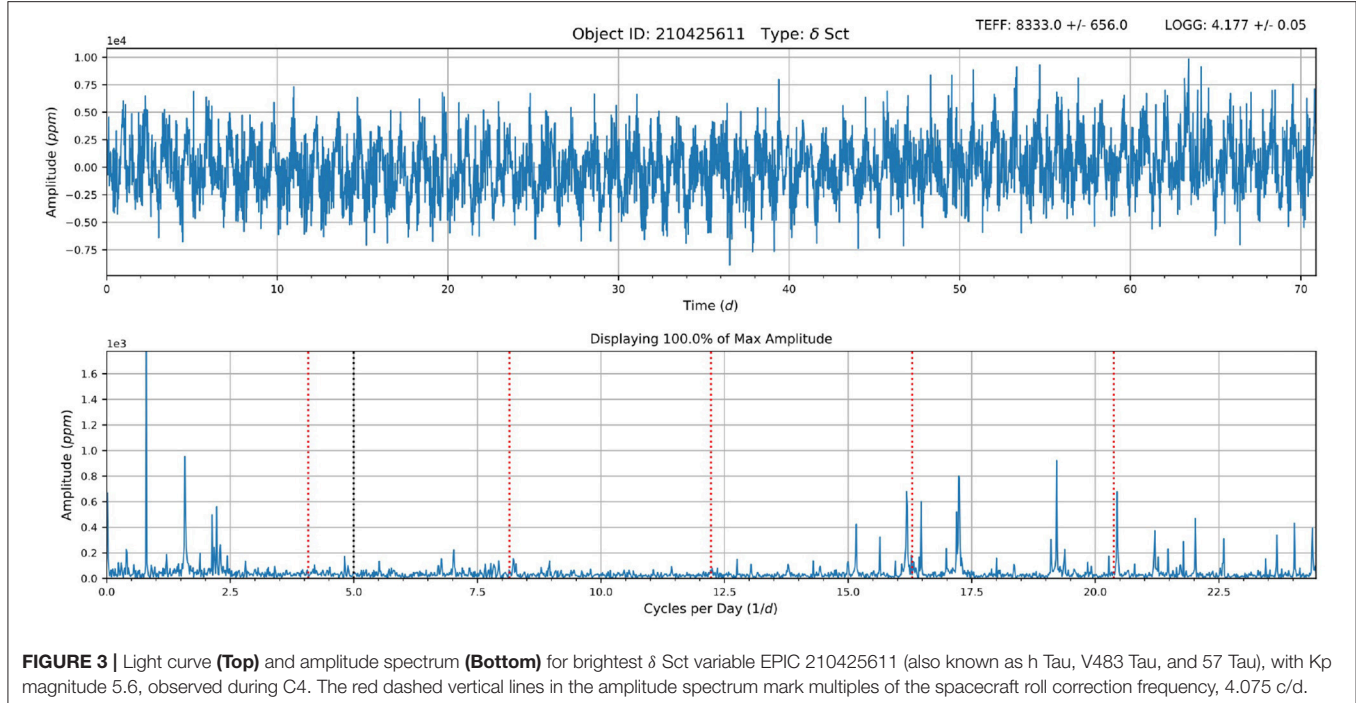


FIGURE 2 | T_{eff} distribution of C8, C11, and C7 targets observed by K2.

Sct candidates varied from 4% (C11) or 5% (C7) down to only 0.15% (C8).

Figure 1 shows spectroscopic Hertzsprung-Russell diagrams, \log surface gravity ($\log g$) vs. T_{eff} , for the C8, C11, and C7 targets, respectively, with the δ Sct candidates shown as red dots. The $\log g$ and T_{eff} are taken from the K2 EPIC catalog (Huber et al., 2017). **Figure 2** shows the T_{eff} distribution of stars in each of these campaigns. We chose to illustrate results of these three campaigns because they represent the extremes in number of δ Sct candidates among the campaigns of Table 1. C8 has the most stars observed (3370), but only five δ Sct candidates (0.15%), primarily because this sample contains mostly stars in the lower main sequence with $T_{\text{eff}} < 6,000$ K that are too cool to be δ Sct variables. The field for C11 (toward the Galactic Center) was so rich that the target list was truncated at magnitude < 13.2 ; therefore, the sample is biased toward hotter and higher-mass main-sequence stars, and has a larger percentage of δ Sct candidates (3.8%). C7 has the smallest number of observed targets (506), but it actually has the largest percentage of δ Sct candidates



(4.5%). This sample contains stars both on the lower main sequence and in the T_{eff} region expected for δ Sct and hybrid stars.

Figures 3–9 show example light curves and amplitude spectra for several δ Sct candidates. **Figure 3** shows the brightest candidate, EPIC 210425611, with Kp magnitude 5.6, observed during C4. This star is the previously known δ Sct variable h Tau,

also known as V483 Tau and 57 Tau (Liakos and Niarchos, 2017). Its amplitude spectrum also shows low-frequency γ Dor-type modes. **Figure 4** shows the light curve and amplitude spectrum for the faintest candidate, EPIC 247333962, with Kp magnitude 15.9, observed during C13. The amplitude spectrum clearly shows several δ Sct frequencies, illustrating that *Kepler* is able to detect pulsations even for very faint targets.

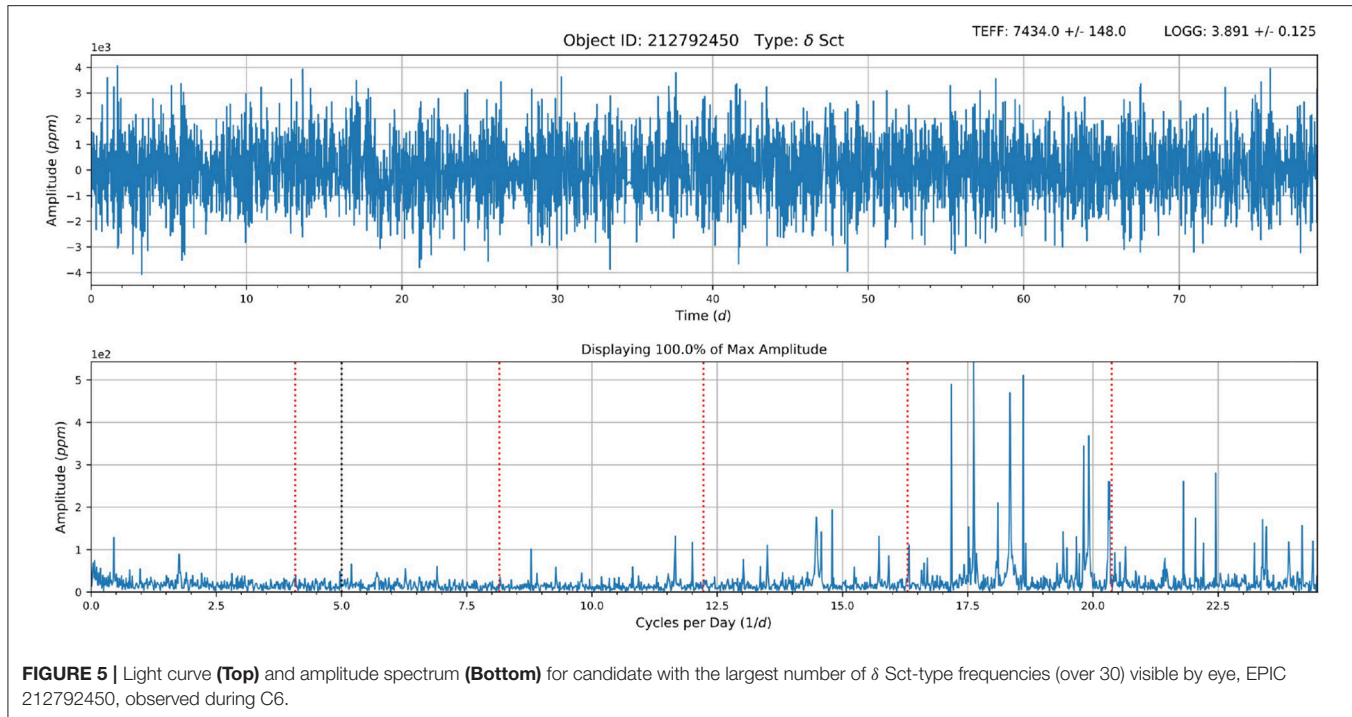


FIGURE 5 | Light curve (**Top**) and amplitude spectrum (**Bottom**) for candidate with the largest number of δ Sct-type frequencies (over 30) visible by eye, EPIC 212792450, observed during C6.

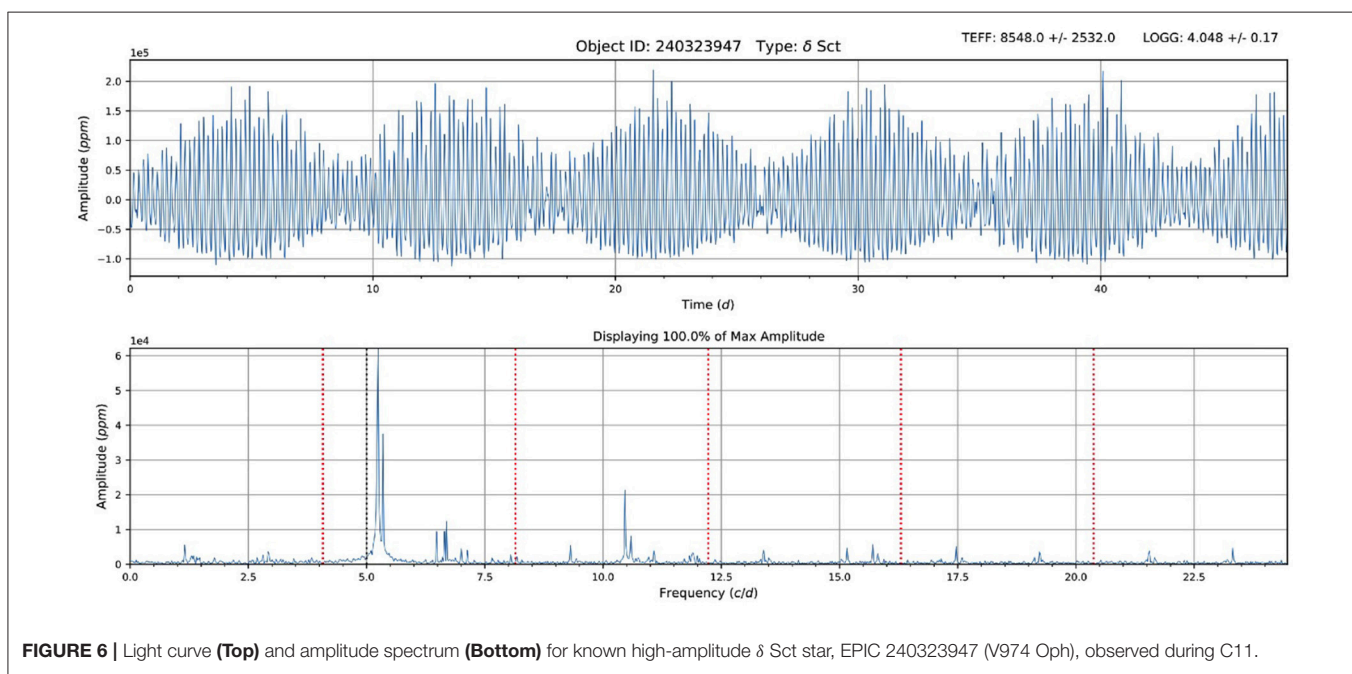


FIGURE 6 | Light curve (**Top**) and amplitude spectrum (**Bottom**) for known high-amplitude δ Sct star, EPIC 240323947 (V974 Oph), observed during C11.

Figure 5 shows the light curve and amplitude spectrum for the candidate with the largest number of δ Sct-type frequencies visible by eye, EPIC 212792450, observed during C6. **Figure 6** shows the highest-amplitude δ Sct variable, EPIC 240323947, observed during C11, with two modes of frequency just above 5 c/d beating against each other. This star is the known high-amplitude δ Sct star V974 Oph (Poretti, 2003).

Figure 7 shows the light curve and amplitude spectrum for the hottest δ Sct candidate, EPIC 233466131, observed during C11.

This star, with EPIC catalog T_{eff} 10,722 K, seems too hot to be a δ Sct variable, but is also too cool to be a β Cep p-mode pulsator. **Figure 8** shows the light curve and amplitude spectrum for the coolest δ Sct candidate, EPIC 235864398, observed during C11. This star has $T_{\text{eff}} = 4950$ K, a low surface gravity ($\log g = 2.68$), and high luminosity, according to the EPIC catalog, and is likely evolving off of the main sequence. Finally, **Figure 9** shows the light curve and amplitude spectrum of a δ Sct candidate in an eclipsing binary, EPIC 247553546, observed during C13.

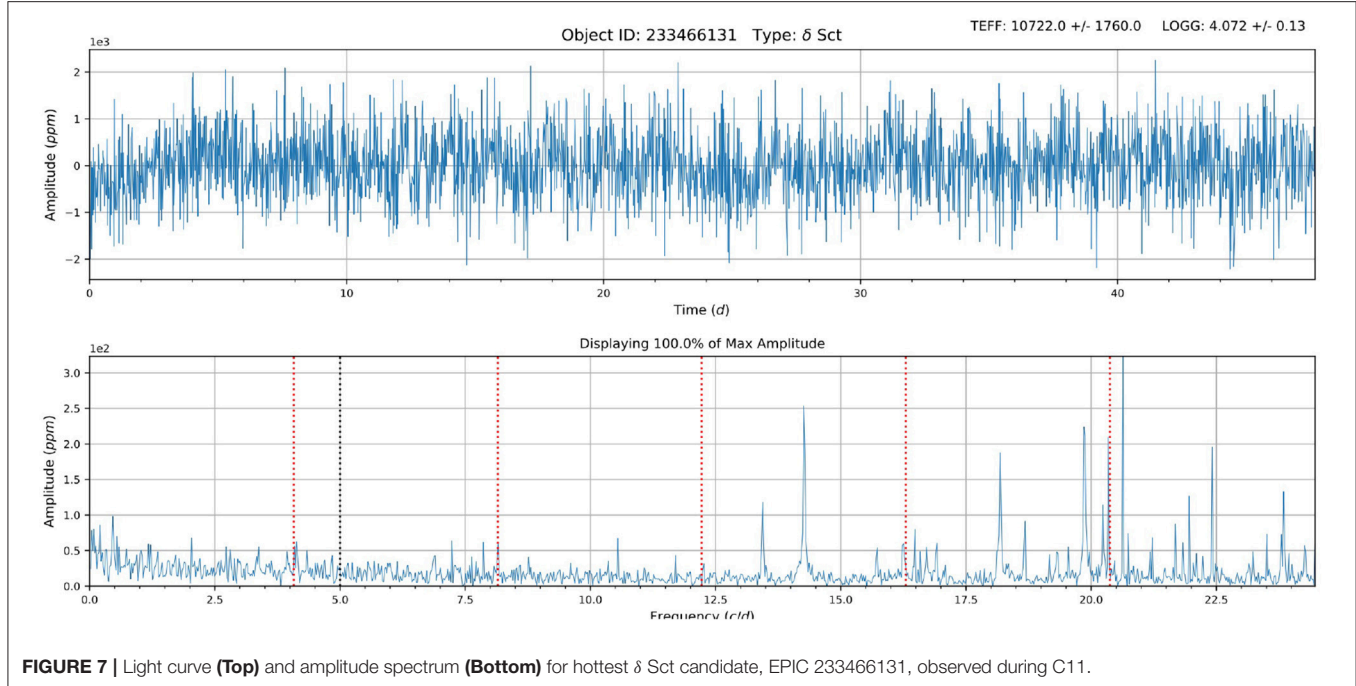


FIGURE 7 | Light curve (**Top**) and amplitude spectrum (**Bottom**) for hottest δ Sct candidate, EPIC 233466131, observed during C11.

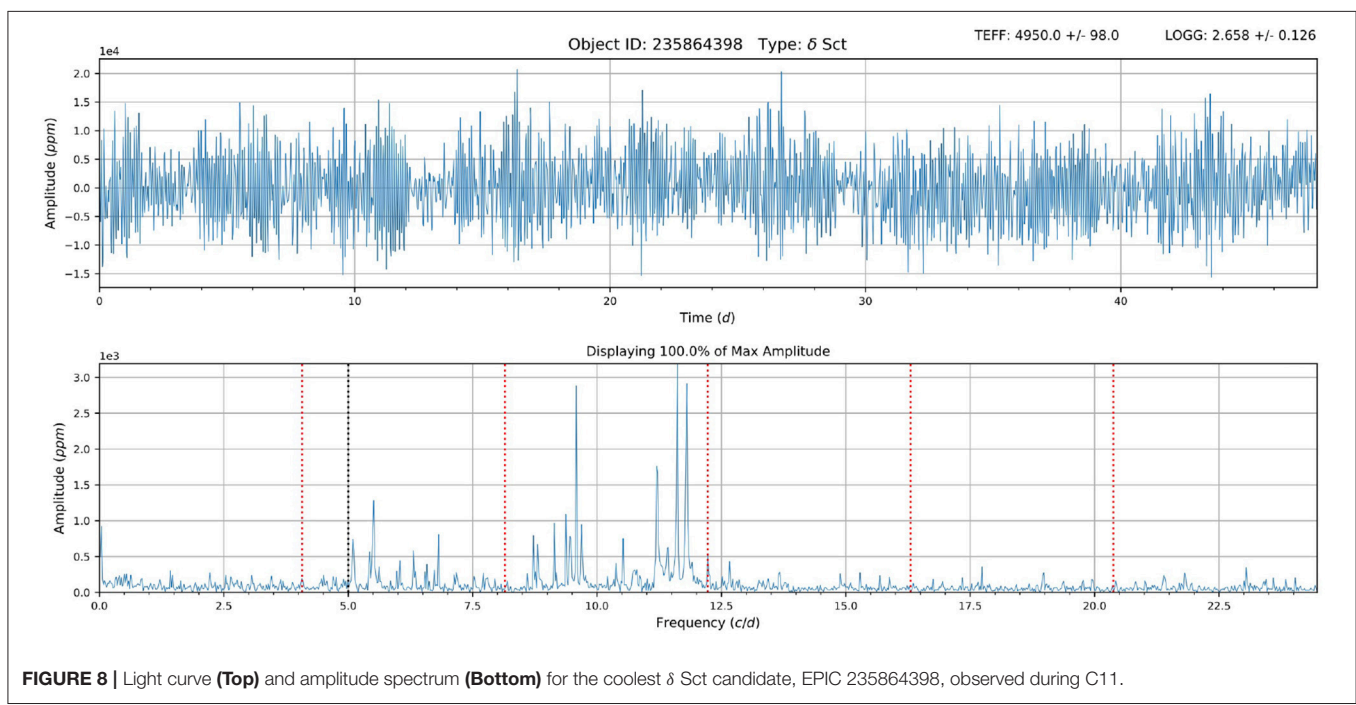


FIGURE 8 | Light curve (**Top**) and amplitude spectrum (**Bottom**) for the coolest δ Sct candidate, EPIC 235864398, observed during C11.

For each of the 249 δ Sct candidates, **Table 2** lists the EPIC catalog number, K_p magnitude, T_{eff} , $\log g$, alternate identifier in the SIMBAD Astronomical Database, number of references to the star in the literature from SIMBAD, and whether it is a known δ Sct variable. Most of the stars with K_p mag < 10 are not referenced beyond the EPIC catalog and have no alternate designation. However, many of the brighter stars have many references, and 17 are known δ Sct variables; these stars may be

excellent candidates for asteroseismic analysis using the *Kepler* data. Not all of the candidates in **Table 2** may turn out to be δ Sct stars. From the pulsation amplitude spectra alone they could be confused with, e.g., p-mode pulsating β Cep variables, or g-mode pulsating subdwarf B variables. However, β Cep variables typically have T_{eff} of around 20,000 K, and so are hotter than the hottest stars in **Table 2**. The sdBV stars have T_{eff} of 20,000–30,000 K, and $\log g \sim 5.2$ –5.8 (Heber, 2016), higher than the stars in

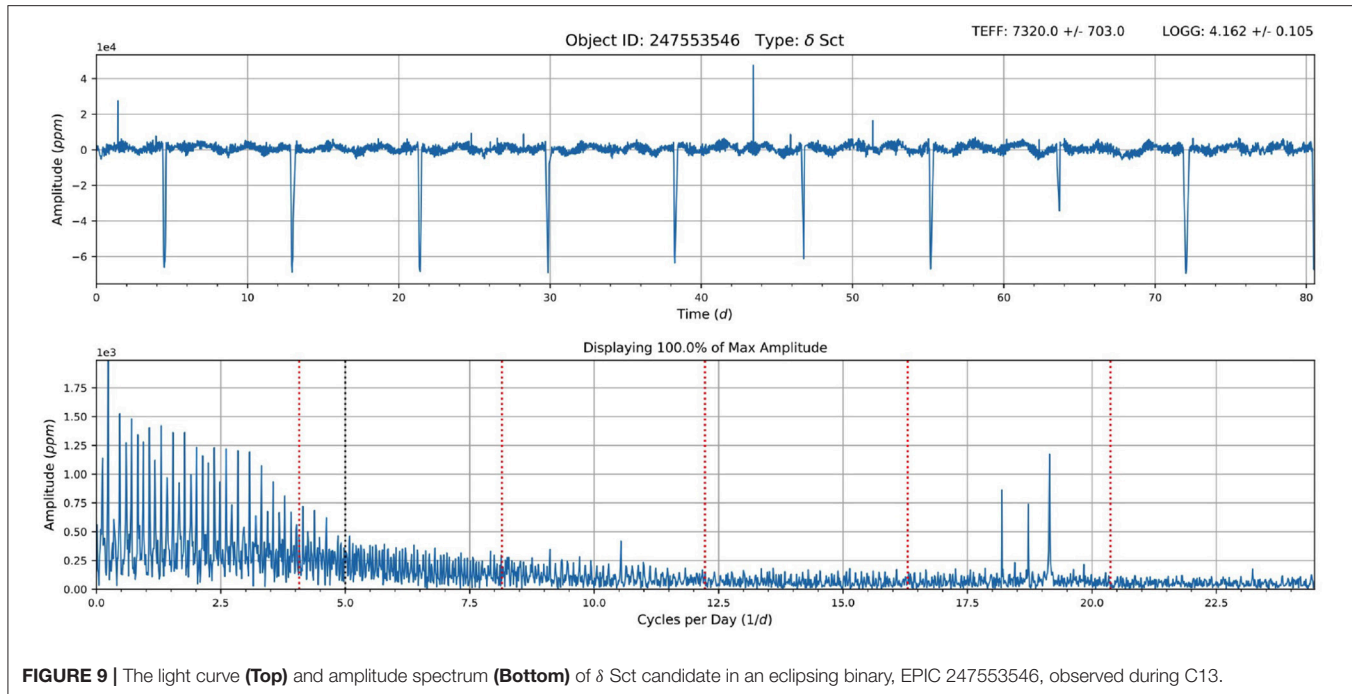


FIGURE 9 | The light curve (**Top**) and amplitude spectrum (**Bottom**) of δ Sct candidate in an eclipsing binary, EPIC 247553546, observed during C13.

Table 2. It is possible that the T_{eff} and $\log g$ of the EPIC catalog are incorrect; Huber et al. (2016) use both color photometry and spectroscopy to derive the EPIC catalog values, taking into account systematic biases uncovered in the original *Kepler* input catalog, and quote uncertainties of $\sim 3\%$ for T_{eff} (i.e., 210 K for a 7,000 K star), and 0.3 dex for $\log g$. It is also possible that the K2 light curve data is contaminated by nearby stars, or that the stars are members of multiplets; deciphering these possibilities will require additional investigations.

Figure 10 shows distributions of properties from the EPIC catalog for the 249 δ Sct candidates. Most of the candidates have K_p magnitude between 8 and 12, but there are a significant number of faint candidates with $K_p > 14$. The T_{eff} distribution peaks at about 7,000 K, as expected for δ Sct variables, but there are a few somewhat hotter and cooler candidates. Most of the stars have metallicity $[\text{Fe}/\text{H}]$ around 0, i.e., near solar; many have metallicities higher than solar, as would be expected for these variable candidates more massive and younger than the Sun. Some stars have a very low $[\text{Fe}/\text{H}]$; these stars could have formed from lower-metallicity material or may be showing abundance anomalies resulting from diffusive settling.

Figure 11 shows a Hertzsprung-Russell diagram of the 249 candidates, based on EPIC catalog luminosity and T_{eff} values. Most of the stars lie along the main sequence, but a few appear to be evolving off of the main sequence. **Figure 11** also shows the mass and distance distributions of the candidates, based again on EPIC catalog values. The mass distribution peaks at about $1.6 M_{\odot}$, typical for δ Sct variables. The distance distribution appears to have a bimodal structure, with most candidates nearby, but some at 1,000–2,000 pc, representing a population perhaps in a distant young cluster or Milky Way spiral arm.

3. RESULTS

For each δ Sct candidate, we counted by eye the number of modes with frequencies between 5 and 24.5 c/d having amplitude greater than about $4 \times$ the local background level. We did not count frequencies that were very close to multiples of the 4.075 c/d (~ 6 hour) spacecraft roll correction frequency marked by red vertical dashed lines on the amplitude spectra (see, e.g., Figures 3–9). We also noted the amplitude and frequency with maximum amplitude, and flagged any candidates with more than one high-amplitude mode with frequency < 5 c/d, indicating a γ Dor/ δ Sct hybrid candidate.

We created a Matlab algorithm to process the light curves, pre-whiten the δ Sct frequencies in order of the highest amplitude modes, and count the number of modes with signal/noise ratio > 6 . The algorithm also searched for frequencies that were multiples of the spacecraft roll correction frequency, as well as frequencies that were combinations of a stellar frequency and the spacecraft roll correction frequency, thereby eliminating some spurious frequencies. Because the algorithm could identify frequencies with lower amplitudes than identifiable by eye, but also could eliminate more artifact combination frequencies, the algorithm sometimes counted more, but also sometimes fewer frequencies than counted by eye. The algorithm results generally agreed with the by-eye determination of the amplitude and frequency of the maximum-amplitude δ Sct mode, although it could quantify these values to higher accuracy than the by-eye estimate. The Matlab algorithm also identified and determined intrinsic and combination frequencies for later use in asteroseismic analyses.

Table 3 summarizes the number of modes with frequency > 5 c/d, and the amplitude and frequency of the maximum-amplitude mode, counted by eye and by using the Matlab script,

TABLE 2 | Summary of properties of δ Sct candidates.

EPIC	Kp mag	T _{eff} (K)	log g	SIMBAD Designation	# Refs.	Known δ Sct
201132898	6.58	7072	3.95	V* FG Vir	205	Yes
201340727	15.58	6058	4.28		1	
203578387	11.39	7523	3.88	TYC 6813-730-1	1	
203676598	10.68	6794	3.73	TYC 6814-1301-1	1	
203690511	10.81	8564	3.61	TYC 6814-473-1	0	
203703889	11.03	6885	4.21	TYC 6813-1078-1	2	
203705702	10.77	7284	4.18	TYC 6813-509-1	1	
203735223	10.34	8457	3.64	HD 152283	4	
203763791	11.14	7000	4.03	TYC 6813-1078-1	1	
203914521	10.92	6767	4.27	CD-24 12899	2	
204019242	8.22	7989	4.17	HD 153172	10	
204053734	11.57	6528	4.05	TYC 6810-898-1	1	
204510816	9.22	6865	3.76	TYC 6230-1594-2	0	
204510921	9.09	6865	3.76	ADS 10251 AB	7	
210425611	5.59	8333	4.18	h Tau	196	Yes
211013743	9.63	7420	4.18	SAO 76387	24	
211018096	8.38	7030	3.85	HD 23791	58	
211040918	8.12	8016	4.31	HD 23512	119	
211044267	7.82	8352	4.18	V* V650 Tau	98	Yes
211057064	8.12	7834	4.19	HD 23863	76	
211080847	9.02	7491	4.14	HD 23325	77	
211088007	8.88	6192	4.00	V* V624 Tau	111	Yes
211115721	8.82	6393	4.00	V* V534 Tau	98	Yes
211909987	8.86	7639	4.05	HD 74589	20	
211914004	7.95	7860	3.65	V* BY Cnc	80	Yes
211931309	8.93	6702	3.96	V* BV Cnc	74	Yes
211935741	8.06	7629	3.87	V* HI Cnc	60	Yes
211936163	6.78	7848	3.58	HD 73210	81	
211945791	7.96	7520	3.93	V* BX Cnc	96	Yes
211953002	8.72	6519	3.86	V* BR Cnc	95	Yes
211957791	8.82	7203	4.13	V* BS Cnc	112	Yes
211979345	8.34	7895	4.16	HD 73872	55	Yes
211995547	9.36	6277	4.00	HD 74058	35	
211995573	8.79	6392	3.90	V* BQ Cnc	78	Yes
212008515	8.85	6851	4.16	HD 74587	22	Yes
212505176	14.27	7604	3.12			
212557497	14.27	7312	3.06			
212628518	8.61	7233	4.15	HD 122370	15	Yes
212792450	9.60	7233	4.12	HD 117674	3	
213674056	11.28	6967	4.03	TYC 6887-1760-1	1	
213814481	9.99	7190	3.96	TYC 6901-160-1	1	
214404873	10.20	6700	3.90	TYC 6881-1650-1	1	
214436324	11.84	6496	4.01			
214623776	11.84	7027	4.16	TYC 6864-722-1	1	
214783113	11.98	6482	4.13			
214892340	9.46	6625	3.69	HD 175757	4	
215076557	11.86	6615	3.83	TYC 6877-302-1	1	
215409060	11.85	7067	3.95	TYC 6874-1073-1	1	
215584718	11.83	6815	4.12	TYC 6873-1116-1	1	

(Continued)

TABLE 2 | Continued

EPIC	Kp mag	T _{eff} (K)	log g	SIMBAD Designation	# Refs.	Known δ Sct
215616052	10.39	7111	4.14	HD 175601	7	
215682566	11.82	7028	4.02			
215953080	11.91	6840	3.92			
216123036	11.90	6696	3.94			
216202250	11.92	7492	3.98			
216308801	11.89	8157	3.94	TYC 6856-47201	1	
216364273	12.20	6297	4.23			
217233339	12.12	7430	3.99	TYC 6295-1147.1	0	
217597196	9.83	8223	3.75	HD 180930	2	
218942345	10.30	7485	3.88	HD 182850	2	
219050824	11.91	6613	4.09			
219062123	10.46	8067	3.78	HD 180668	2	
219112324	10.37	7774	3.90	HD 177636	2	
220238863	15.75	6210	4.37			
220369033	7.14	6876	3.76	HD 5143	43	
220379315	8.01	7505	3.70	HD 5655	11	
220492184	8.04	7142	3.63	HD 9648	16	
220617956	8.52	7533	3.97	TYC 605-302-1	20	
221514420	10.54	6426	3.73	HD 316146	2	
221597630	10.76	6581	3.78	HD 316218	2	
221835782	9.81	8484	3.97	HD 160122	3	
223461917	10.09	7612	3.99	HD 161737	2	
223485618	10.89	7167	4.03	HD 314726	2	
224720218	10.25	6698	3.76	HD 159615	2	
224938189	10.71	7326	3.88	CPD-23 6621	1	
225048843	9.55	6563	3.93	HD 159933	2	
225119740	9.47	6201	3.97	HD 158721	4	
225406132	8.10	6748	3.76	HD 159894	15	
225618802	11.02	6790	4.07	CPD-22 6404	1	
226256676	7.99	6804	3.57	HD 159663	12	
226339600	10.78	8719	3.89	HD 159274	4	
226353331	11.46	6236	3.87	TYC 6246-340-1	0	
226401681	11.59	6526	4.02	TYC 6247-298-1	0	
226458042	12.68	5317	2.48			
227606751	11.32	6927	4.13	TYC 6239-921-1	0	
228705808	8.41	7366	4.19	HD 91168	15	
228705867	7.97	7577	4.17	** STF 1649	0	
228922952	8.83	7201	4.15	HD 110614	5	
230194154	7.80	7025	3.99	HD 154214	3	
230611120	11.53	7360	4.04	TYC 6244-628-1	0	
230616631	8.51	7057	3.57	HD 154965	5	
230631967	10.41	7516	4.20	BD-20 4647	1	
230648601	10.20	6617	3.74	CPD-20 6471	1	
230649783	10.22	6474	3.80	BD-20 4652	1	
230652057	11.36	6795	3.76	TYC 6240-748-1	0	
230653899	11.19	6864	3.73	CPD-20 6464	1	
230826613	11.24	7101	4.03	TYC 6236-1406-1	0	
230867465	11.19	6751	3.92	TYC 6236-1391-1	0	
230961039	10.17	7020	3.89	TYC 6814-1381-1	0	
230995585	8.16	7496	3.82	HD 154241	17	

(Continued)

TABLE 2 | Continued

EPIC	K _p mag	T _{eff} (K)	log g	SIMBAD Designation	# Refs.	Known δ Sct
231081322	8.27	8105	3.82	HD 155143	5	
231081534	8.69	8232	4.02	CD-24 13177B	2	
231190822	9.60	7595	4.22	CD-24 122998A	2	
231191024	10.14	8081	4.07	HD 153335	2	
231278798	9.98	7713	4.10	HD 154946	2	
231282136	9.99	7347	3.66	HD 155126	2	
231285847	8.47	7471	3.61	HD 153460	7	
231452640	8.92	7005	4.21	HD 155142	5	
231812289	11.87	7536	4.03	TYC 6823-1296-1	0	
231836923	10.10	6963	4.13	HD 154993	1	
232031620	7.91	7876	4.12	HD 152989	8	
232176025	8.16	9871	3.65	HD 153636	1	
232218434	10.02	7781	3.95	HD 153568	4	
233129558	12.19	7161	3.84	TYC 7361-755-1	0	
233193088	7.91	8596	4.15	HD 154978	2	
233422493	9.91	7546	3.65	HD 157897	4	
233434079	9.71	7034	4.24	HD 156683	7	
233463757	8.30	7205	4.00	HD 155468	7	
233466131	10.09	10722	4.07	HD 157859	3	
233466773	10.89	7146	3.86	TYC 6238-535-1	0	
233553924	10.67	8035	4.10	TYC 6238-3049-1	0	
234109260	10.07	6917	3.72	HD 157001	2	
234138507	9.46	7540	4.02	HD 156463	4	
234201903	8.63	7869	3.61	HD 156542	12	
234218726	9.97	7538	4.20	HD 157055	4	
234247882	9.42	7133	4.07	HD 155927	8	
234713455	10.64	7750	3.70	CPD-25 5990	1	
234854390	8.98	6994	3.90	HD 155430	7	
234876533	8.49	7637	4.14	HD 155491	3	
235206885	12.35	6140	4.17			
235219917	10.67	8247	3.89	CPD-23 6527	1	
235231827	11.38	6838	3.68	TYC 6812-685-1	0	
235252324	11.38	6971	4.07	TYC 6825-513-1	0	
235263502	11.42	6821	4.04	CD-23 13372	1	
235268020	11.82	7257	4.04	TYC 6812-490-1	0	
235285649	12.41	4894	2.67			
235288870	11.31	7431	3.74	CD-23 13335	1	
235297752	10.96	6988	3.57	CD-23 13317	1	
235326610	11.30	7001	4.16	CD-23 13374	1	
235863134	9.58	6785	3.80	HD 155517	4	
235864398	10.07	4950	2.66	TYC 6824-68-1	0	
235961804	11.18	7650	3.67	CPD-28 5583	1	
236025929	11.04	7531	3.94	HD 315790	2	
236076864	10.84	6693	3.61	CPD-28 5638	1	
236250262	10.98	6533	3.82			
236311085	11.67	6511	3.89	TYC 6834-71-1	0	
236338125	11.10	6498	4.21	CPD-27 5660	1	
236420722	11.46	8643	3.74	TYC 6833-111-1	0	
237711874	11.14	7095	4.19	TYC 7362-163-1	0	
237719954	11.44	6656	4.01	TYC 7362-236-1	0	

(Continued)

TABLE 2 | Continued

EPIC	Kp mag	T _{eff} (K)	log g	SIMBAD Designation	# Refs.	Known δ Sct
237768774	11.64	6988	3.88	TYC 7362-18301	0	
237911727	9.48	6474	3.86	HD 156320	2	
237944799	8.83	7094	3.61	HD 156117	5	
237969415	8.39	7857	4.15	HD 155868	5	
237987964	6.31	9785	4.15	HD 155940	21	
240292657	11.09	7224	3.59	HD 316096	2	
240296875	10.79	6680	3.77	HD 316155	2	
240323947	11.51	8548	4.05	V* V974 Oph	24	Yes
240378036	10.82	8140	3.99	CPD-29 4729	1	
240642822	11.08	7790	3.58	HD 315795	3	
240686489	10.48	6566	3.63	CPD-28 5663	1	
242088649	9.24	7345	4.02	TYC 7375-608-2	0	
242088762	8.82	7345	4.02	TYC 7375-608-1	0	
242099103	11.37	7426	3.81	HD 315868	1	
242138878	10.98	7660	3.85	HD 316026	1	
242171743	9.78	7421	3.67	HD 159723	3	
245910293	8.53	7494	4.06	HD 221180	10	
245984590	9.85	7154	3.79	HD 221446	3	Yes
246029438	11.47	7934	4.12	BD-09 6273	0	
246031849	7.53	7644	4.06	HD 220109	5	
246094180	8.28	7072	3.95	HD 218475	9	
246101155	7.83	7555	3.86	HD 221925	14	
246123792	8.15	7775	3.62	HD 220036	2	
246130239	8.67	7489	4.11	HD 220185	5	
246228220	7.61	7816	4.19	HD 223215	2	
246235560	8.96	6660	3.87	HD 218835	5	
246295525	13.63	7584	3.11			
246351401	9.10	6763	4.02	HD 218953	6	
246390686	9.76	7652	4.06	HD 218834	1	
246448276	10.19	7015	4.16	TYC 577-291-1	0	
246460499	7.54	8072	4.13	HD 219114	5	
246755448	15.05	7094	4.16			
246765955	10.81	7556	4.06	HD 286096	1	
246792876	10.51	7931	4.04	TYC 1282-1865-1	0	
246889963	14.34	7457	4.15	PM2000 224251	2	
246892566	14.46	7092	4.15	PM2000 227650	2	
246895097	8.60	8944	3.87	HD 29727	9	
246952727	9.03	7764	3.74	CDDM J05122+1716AB	1	
246969097	15.15	6803	4.19			
247227122	6.17	5863	3.22	HD 29104	38	
247236218	8.41	5279	2.49	HD 31325	0	
247244984	15.36	6433	4.21			
247249443	14.49	7217	4.17			
247251791	15.81	5987	4.30			
247255798	15.80	6648	4.21			
247261516	13.61	6616	4.03			
247264515	15.89	7495	4.19			
247268706	14.48	6649	4.14			
247278455	14.29	7944	4.12			

(Continued)

TABLE 2 | Continued

EPIC	K _p mag	T _{eff} (K)	log g	SIMBAD Designation	# Refs.	Known δ Sct
247292095	15.54	6541	4.21			
247295392	15.19	6412	4.20			
247319900	15.87	6094	4.29			
247321564	10.14	8676	4.01	TYC 1278-1709-1	0	
247333962	15.89	6361	4.23			
247338349	15.39	6256	4.24			
247382496	15.51	6164	4.29			
247382770	15.70	6837	4.18			
247383620	13.59	6238	4.24			
247465892	15.84	6477	4.22			
247473022	15.45	6850	4.20			
247473204	15.14	7533	4.17			
247481643	14.94	6580	4.20			
247504599	14.76	6490	4.23			
247505615	14.35	6838	4.12			
247511123	15.84	6057	4.28			
247526175	14.68	6432	4.21			
247544254	15.10	6213	4.22			
247553546	15.19	7320	4.16			
247576531	15.47	6407	4.23			
247584516	7.55	7532	3.81	HD 28621	11	
247598095	13.06	6935	4.16			
247606589	15.71	6707	4.19	LAMOST J050309.73+225954.2	1	
247608052	14.23	6686	4.20			
247648610	9.10	6869	3.70	HD 30231	5	
247650349	15.66	7302	4.18			
247676134	13.71	7169	4.14			
247698817	12.78	7378	4.11	GJGTZ 52762	3	
247700654	15.67	6310	4.24			
247702571	9.41	6911	3.64	HD 284527	2	
247708413	15.13	6448	4.20	GJGTZ 49758	2	
247708505	13.96	6489	4.33	GJGTZ 49606	2	
247714857	14.24	6167	4.28			
247743444	15.70	6285	4.25			
247749294	15.64	6134	4.29			
247760775	14.16	6867	4.14	[Tzs98] 62	1	
247764363	7.79	7277	3.66	HD 31880	17	
247766003	15.71	6409	4.22			
247768006	15.89	6531	4.21			
247770898	15.83	6413	4.20			
247811337	15.67	6362	4.22			
247828212	15.32	6750	4.16			
247841082	15.77	6027	4.37	[HH95] V1062 Tau-57		
247877340	15.79	6668	4.19			
247899700	14.62	5957	4.13			
247917882	6.26	8883	3.97	HD 29459	36	
247931858	15.66	6703	4.18			
248122534	15.03	7543	4.15			
248125694	15.63	6378	4.19			
248186557	14.37	6366	4.12			
248264996	11.45	6925	3.99	TYC 1844-954-1	0	

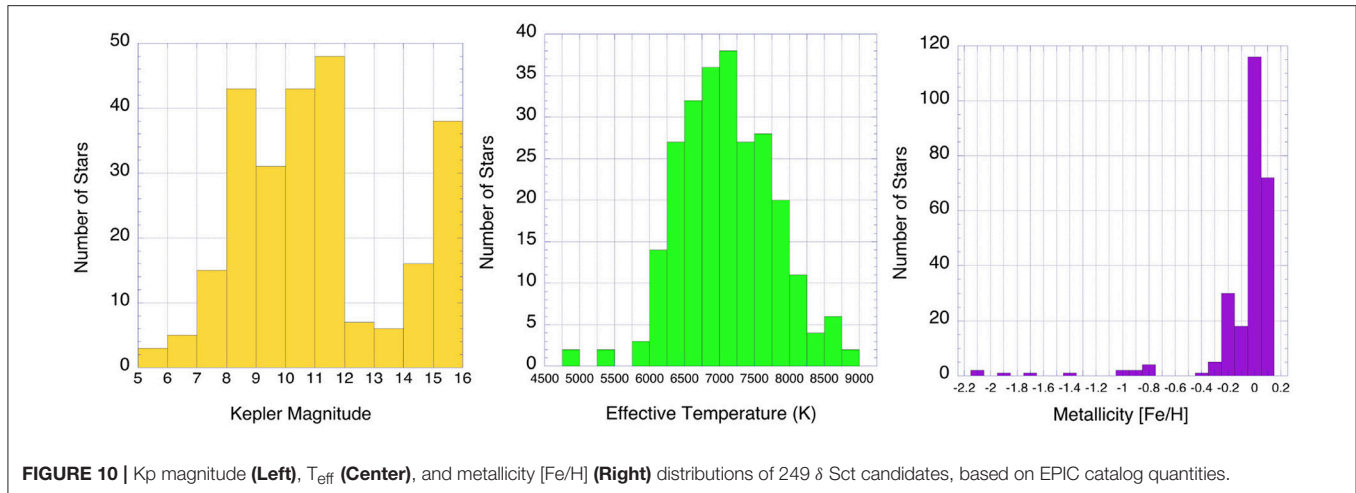


FIGURE 10 | K_p magnitude (**Left**), T_{eff} (**Center**), and metallicity $[\text{Fe}/\text{H}]$ (**Right**) distributions of 249 δ Sct candidates, based on EPIC catalog quantities.

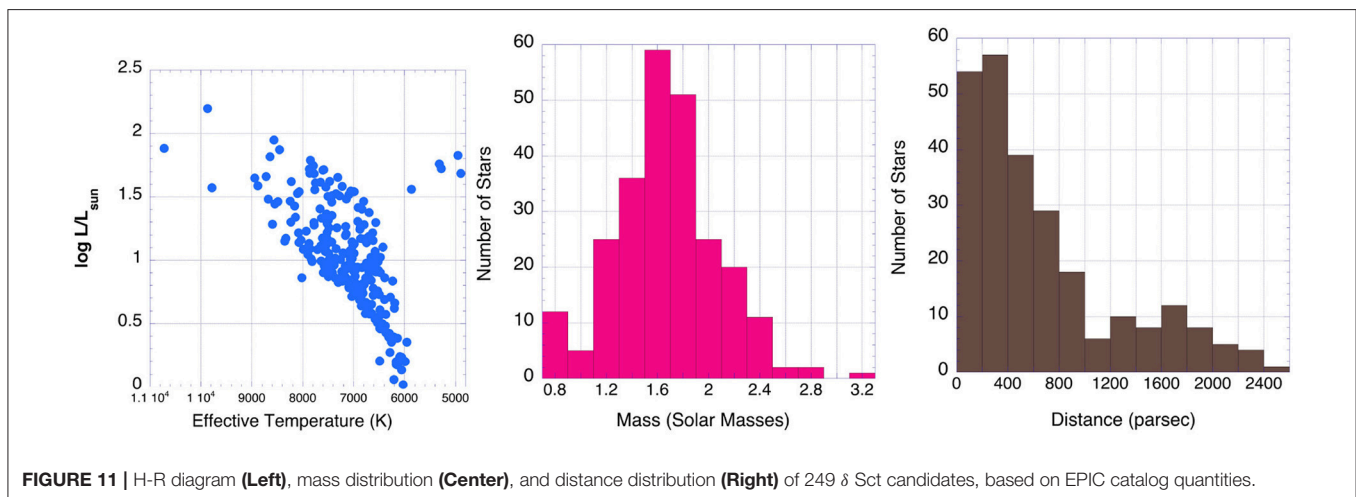


FIGURE 11 | H-R diagram (**Left**), mass distribution (**Center**), and distance distribution (**Right**) of 249 δ Sct candidates, based on EPIC catalog quantities.

for the 249 candidate δ Sct stars. The Table also flags the stars showing more than one low-frequency (< 5 c/d) mode that are hybrid candidates.

Figure 12 plots the distribution of the number of frequencies per star > 5 c/d (counted by eye), the distribution of amplitudes of highest-amplitude modes (excluding the two highest-amplitude candidates), and the distribution of frequencies having maximum amplitude for the 249 candidates. Most of the candidates have < 10 δ Sct modes, but some show more than 30 modes by eye, and up to 100 modes when counted using the Matlab algorithm; therefore these stars may yield the most useful constraints for asteroseismic studies. Most of the stars have maximum-amplitude mode < 2 parts per thousand that would be difficult to detect without long time-series, high-precision photometry such as obtained by *Kepler*. There does not seem to be any preferred frequency with maximum amplitude in the 5–24.5 c/d frequency range.

Figure 13 shows the number of frequencies counted by eye vs. the number found using the Matlab algorithm; as discussed earlier the Matlab pre-whitening algorithm is able to identify a larger number of significant frequencies, but also is able to find and remove more artifact frequencies. The middle panel shows

the distribution of the number of frequencies > 5 c/d per star vs. T_{eff} , and the last panel shows the distribution of amplitude of the maximum-amplitude frequency vs. T_{eff} . It appears that stars with the largest amplitudes and the largest number of frequencies are found in the middle of the temperature range at about 7,000 K, i.e., in the middle of the δ Sct instability region.

4. CONCLUSIONS

Kepler has obtained unprecedented long time-series high signal-to-noise photometric data enabling the discovery and characterization of variable stars pulsating in many simultaneous radial and non-radial modes. We have identified 249 obvious δ Sct candidates so far in light curves collected as part of our K2 Guest Observer proposals for 11 (out of 19) campaigns of K2. Seventeen of these stars were already known as δ Sct stars, according to the SIMBAD database. 126 out of 249 candidates show low frequencies < 5 c/d and may be hybrid γ Dor/ δ Sct pulsators. We do not find any correlations between pulsation properties (e.g., number of frequencies, frequency with maximum amplitude, etc.) and stellar properties (e.g., T_{eff} , $\log g$, . . .), as listed in the EPIC catalog.

TABLE 3 | Summary of pulsation properties of δ Sct candidates^a.

EPIC	Kp mag	T _{eff} (K)	# Freqs.	# Freqs. ^M	A _{max} (ppm)	A _{max} ^M (ppm)	v _{A_{max}} (c/d)	v _{A_{max}} ^M (c/d)	Hybrid flag
201132898	6.58	7072	5	7	1.6E+04	1.60E+04	12.7	12.72	1
201340727	15.58	6058	2	2	7.0E+02	6.80E+02	23.0	21.53	0
203578387	11.39	7523	13	29	4.5E+03	5.04E+03	15.0	14.94	0
203676598	10.68	6794	10	19	3.0E+02	3.90E+02	14.2	16.56	1
203690511	10.81	8564	30	39	9.2E+02	1.19E+03	12.0	10.85	1
203703889	11.03	6885	13	8	4.0E+02	4.54E+02	17.7	17.85	1
203705702	10.77	7284	5	7	1.2E+03	1.38E+03	21.3	21.35	0
203735223	10.34	8457	4	6	3.0E+02	4.18E+02	10.1	10.10	1
203763791	11.14	7000	25	28	2.6E+03	2.58E+03	11.3	11.36	1
203914521	10.92	6767	11	28	5.0E+02	5.99E+02	18.2	19.95	1
204019242	8.22	7989	20	22	1.2E+03	1.45E+03	16.7	16.71	1
204053734	11.57	6528	20	14	1.0E+03	1.24E+03	15.4	15.32	1
204510816	9.22	6865	9	11	1.4E+03	1.73E+03	17.0	16.99	0
204510921	9.09	6865	9	11	1.4E+03	1.55E+03	17.0	16.99	0
210425611	5.59	8333	21	24	9.2E+02	1.24E+03	19.2	17.25	1
211013743	9.63	7420	3	7	9.8E+01	9.92E+01	9.3	9.35	1
211018096	8.38	7030	31	29	3.4E+02	4.69E+02	20.9	20.89	1
211040918	8.12	8016	2	5	2.8E+01	2.92E+01	23.1	23.00	0
211044267	7.82	8352	19	24	1.6E+03	1.61E+03	17.0	17.04	1
211057064	8.12	7834	14	20	5.0E+02	7.54E+02	17.9	17.88	0
211080847	9.02	7491	15	20	5.4E+02	5.67E+02	23.0	23.23	0
211088007	8.88	6192	6	38	4.3E+02	4.99E+02	21.0	20.98	0
211115721	8.82	6393	20	21	7.2E+02	6.13E+02	21.8	20.23	1
211909987	8.86	7639	25	16	7.0E+02	7.82E+02	23.9	20.58	0
211914004	7.95	7860	14	21	2.5E+03	2.00E+03	18.3	21.39	1
211931309	8.93	6702	25	36	1.2E+03	1.34E+03	16.5	16.45	0
211935741	8.06	7629	20	14	1.3E+03	1.49E+03	20.6	23.64	0
211936163	6.78	7848	16	21	1.0E+03	1.59E+03	12.2	12.12	1
211945791	7.96	7520	24	26	1.8E+03	2.11E+03	22.6	23.86	1
211953002	8.72	6519	15	17	2.2E+03	2.55E+03	23.9	23.97	0
211957791	8.82	7203	12	29	3.1E+03	3.76E+03	17.0	17.04	0
211979345	8.34	7895	31	27	3.6E+02	4.96E+02	22.8	15.53	1
211995547	9.36	6277	5	29	5.5E+01	6.04E+01	6.8	6.82	1
211995573	8.79	6392	7	70	1.3E+03	1.17E+03	15.6	15.59	0
212008515	8.85	6851	20	28	1.7E+03	1.87E+03	17.0	17.04	0
212505176	14.27	7604	11	10	1.5E+03	1.59E+03	21.8	21.77	1
212557497	14.27	7312	8	14	3.3E+03	3.41E+03	16.4	16.42	1
212628518	8.61	7233	3	6	3.5E+03	3.88E+03	15.6	15.60	1
212792450	9.60	7233	34	30	5.5E+02	6.80E+02	17.7	18.35	1
213674056	11.28	6967	14	34	3.0E+03	3.17E+03	12.5	12.56	0
213814481	9.99	7190	7	46	2.8E+03	3.96E+03	14.4	14.38	1
214404873	10.20	6700	9	20	5.0E+03	7.16E+03	8.7	8.84	0
214436324	11.84	6496	9	27	2.7E+03	3.65E+03	9.2	9.21	0
214623776	11.84	7027	8	21	1.8E+03	1.17E+03	6.6	6.68	1
214783113	11.98	6482	5	68	7.8E+02	8.75E+02	17.2	17.33	1
214892340	9.46	6625	1	7	1.1E+02	1.36E+02	19.4	19.35	0
215076557	11.86	6615	7	11	5.5E+02	5.86E+02	22.9	22.88	0
215409060	11.85	7067	1	105	6.0E+02	6.21E+02	8.0	7.84	1

(Continued)

TABLE 3 | Continued

EPIC	Kp mag	T _{eff} (K)	# Freqs.	# Freqs. ^M	A _{max} (ppm)	A _{max} ^M (ppm)	v _{A_{max}} (c/d)	v _{A_{max}} ^M (c/d)	Hybrid flag
215584718	11.83	6815	8	12	4.5E+03	4.50E+03	20.2	20.17	1
215616052	10.39	7111	3	17	2.2E+02	2.81E+02	14.6	7.35	1
215682566	11.82	7028	15	33	1.8E+03	2.31E+03	14.2	14.20	0
215953080	11.91	6840	1	16	4.5E+02	4.62E+02	15.5	15.51	0
216123036	11.90	6696	9	20	7.2E+02	8.71E+02	15.1	15.09	1
216202250	11.92	7492	1	5	1.5E+03	1.50E+03	10.8	10.89	0
216308801	11.89	8157	13	21	1.2E+03	1.24E+03	17.7	17.68	0
216364273	12.20	6297	4	53	2.0E+03	2.46E+03	20.8	20.80	1
217233339	12.12	7430	4	9	3.5E+02	3.54E+02	23.8	23.23	1
217597196	9.83	8223	22	30	6.0E+03	6.56E+03	9.0	8.96	0
218942345	10.30	7485	15	27	1.1E+03	1.09E+03	17.0	16.96	0
219050824	11.91	6613	2	6	1.2E+03	1.24E+03	17.8	17.90	0
219062123	10.46	8067	23	26	1.2E+03	1.52E+03	23.1	23.09	0
219112324	10.37	7774	32	40	5.5E+02	5.55E+02	24.1	24.36	0
220238863	15.75	6210	8	7	1.1E+04	1.11E+04	23.5	23.68	1
220369033	7.14	6876	3	19	4.8E+02	6.28E+02	5.9	5.89	1
220379315	8.01	7505	23	34	2.5E+03	3.67E+03	12.0	11.99	1
220492184	8.04	7142	10	16	3.5E+02	5.07E+02	23.2	23.20	1
220617956	8.52	7533	3	64	4.0E+02	4.72E+02	15.2	16.60	1
221514420	10.54	6426	15	14	5.0E+03	5.04E+03	10.1	10.07	1
221597630	10.76	6581	5	8	3.1E+03	3.17E+03	10.0	9.96	1
221835782	9.81	8484	4	5	1.8E+02	1.83E+02	22.4	22.35	0
223461917	10.09	7612	2	6	7.0E+01	7.27E+01	21.3	21.25	1
223485618	10.89	7167	3	6	1.3E+02	1.44E+02	19.6	6.50	0
224720218	10.25	6698	19	27	4.8E+03	5.76E+03	9.2	9.11	0
224938189	10.71	7326	8	15	4.0E+03	4.64E+03	9.7	9.63	1
225048843	9.55	6563	15	18	3.2E+02	4.27E+02	13.7	13.64	1
225119740	9.47	6201	4	15	8.0E+03	8.24E+03	10.4	10.32	1
225406132	8.10	6748	11	26	3.3E+03	4.21E+03	14.0	14.02	0
225618802	11.02	6790	10	13	5.3E+02	5.90E+02	14.8	19.76	0
226256676	7.99	6804	7	19	3.8E+02	3.31E+02	7.5	7.47	1
226339600	10.78	8719	8	7	1.2E+02	1.34E+02	7.1	6.07	1
226353331	11.46	6236	13	11	4.5E+03	5.78E+03	14.0	13.95	1
226401681	11.59	6526	4	6	1.8E+03	1.85E+03	21.9	21.87	0
226458042	12.68	5317	30	19	1.0E+03	1.10E+03	16.8	16.84	0
227606751	11.32	6927	20	22	1.2E+03	1.21E+03	17.4	16.87	0
228705808	8.41	7366	2	22	9.0E+02	1.24E+03	5.3	5.23	0
228705867	7.97	7577	2	24	9.0E+02	8.13E+02	5.3	5.23	1
228922952	8.83	7201	8	10	1.1E+03	1.06E+03	16.4	16.35	0
230194154	7.80	7025	8	28	9.2E+02	9.28E+02	9.7	9.67	1
230611120	11.53	7360	9	15	1.7E+03	1.72E+03	18.2	18.20	0
230616631	8.51	7057	9	56	1.0E+03	1.13E+03	5.3	5.30	1
230631967	10.41	7516	7	10	3.8E+02	4.82E+02	14.8	19.74	0
230648601	10.20	6617	8	13	8.0E+02	8.75E+02	14.6	14.60	0
230649783	10.22	6474	4	19	6.1E+02	2.48E+02	15.6	9.72	1
230652057	11.36	6795	10	20	1.9E+03	2.14E+03	18.8	18.86	0
230653899	11.19	6864	8	11	1.9E+03	1.93E+02	20.4	20.30	1
230826613	11.24	7101	5	8	3.5E+03	3.99E+03	24.3	24.32	0
230867465	11.19	6751	9	9	7.2E+01	7.89E+01	16.2	12.31	0
230961039	10.17	7020	9	17	1.3E+04	1.31E+04	8.6	8.55	0

(Continued)

TABLE 3 | Continued

EPIC	Kp mag	Teff (K)	# Freqs.	# Freqs. ^M	A _{max} (ppm)	A _{max} ^M (ppm)	v _{A_{max}} (c/d)	v _{A_{max}} ^M (c/d)	Hybrid flag
230995585	8.16	7496	8	9	7.1E+03	8.97E+03	8.3	8.04	0
231081322	8.27	8105	8	17	4.2E+03	4.21E+03	14.7	14.80	0
231081534	8.69	8232	6	14	4.2E+03	4.32E+03	14.7	14.80	0
231190822	9.60	7595	7	21	1.2E+03	1.22E+03	15.7	15.75	1
231191024	10.14	8081	5	7	2.0E+03	1.98E+03	15.7	15.75	1
231278798	9.98	7713	21	10	8.1E+02	1.14E+03	23.6	23.68	1
231282136	9.99	7347	14	16	2.7E+03	3.60E+03	6.9	6.89	1
231285847	8.47	7471	22	18	1.8E+03	1.74E+03	18.9	18.92	1
231452640	8.92	7005	6	13	1.1E+02	1.66E+02	7.4	7.36	0
231812289	11.87	7536	6	5	7.8E+02	9.23E+02	22.0	21.96	0
231836923	10.10	6963	8	27	6.5E+02	5.43E+02	15.5	4.86	1
232031620	7.91	7876	7	20	1.3E+03	1.58E+03	18.9	18.80	0
232176025	8.16	9871	7	21	1.8E+02	2.48E+02	8.4	8.32	1
232218434	10.02	7781	10	8	1.2E+02	1.06E+02	11.7	11.68	1
233129558	12.19	7161	7	13	8.1E+03	8.43E+03	22.4	22.39	0
233193088	7.91	8596	9	15	1.4E+03	1.67E+03	23.2	23.56	1
233422493	9.91	7546	3	28	2.0E+02	2.51E+02	7.7	7.73	1
233434079	9.71	7034	6	21	3.0E+02	2.90E+02	6.7	4.92	1
233463757	8.30	7205	8	10	8.2E+02	1.21E+03	17.4	17.39	1
233466131	10.09	10722	17	9	3.2E+02	3.44E+02	20.7	19.87	0
233466773	10.89	7146	16	26	3.0E+02	3.89E+03	7.7	7.73	0
233553924	10.67	8035	25	25	9.0E+02	9.44E+02	15.6	14.90	0
234109260	10.07	6917	8	10	2.5E+02	3.68E+02	7.4	7.27	1
234138507	9.46	7540	5	14	8.0E+02	1.05E+03	21.5	21.46	1
234201903	8.63	7869	5	18	1.8E+04	1.97E+04	7.2	7.08	1
234218726	9.97	7538	6	5	3.7E+02	5.14E+02	14.7	14.77	0
234247882	9.42	7133	15	19	1.1E+03	1.16E+03	20.0	20.07	0
234713455	10.64	7750	1	3	1.2E+02	1.26E+02	21.0	20.97	1
234854390	8.98	6994	4	29	7.5E+02	9.74E+02	19.1	19.05	1
234876533	8.49	7637	19	17	1.6E+03	1.67E+03	13.7	13.67	0
235206885	12.35	6140	7	20	6.2E+02	6.37E+02	11.8	11.83	1
235219917	10.67	8247	6	6	1.2E+02	1.41E+02	18.3	14.21	0
235231827	11.38	6838	12	6	2.5E+02	3.28E+02	20.2	22.95	0
235252324	11.38	6971	1	5	3.2E+02	3.23E+02	15.7	15.83	0
235263502	11.42	6821	10	11	2.0E+03	1.93E+03	18.5	19.44	0
235268020	11.82	7257	1	16	8.0E+02	9.12E+02	13.5	13.53	1
235285649	12.41	4894	7	10	3.5E+02	3.49E+02	10.7	10.72	0
235288870	11.31	7431	7	9	3.6E+02	4.21E+02	17.1	17.08	0
235297752	10.96	6988	6	11	5.2E+03	7.33E+03	8.0	7.98	0
235326610	11.30	7001	5	12	8.5E+01	1.14E+02	5.7	5.80	1
235863134	9.58	6785	17	19	5.0E+02	5.32E+02	16.5	16.51	1
235864398	10.07	4950	16	26	3.2E+03	3.87E+03	11.6	11.80	0
235961804	11.18	7650	4	3	3.5E+02	3.66E+02	15.8	15.73	1
236025929	11.04	7531	2	5	1.8E+02	2.29E+02	10.4	10.37	1
236076864	10.84	6693	4	19	1.8E+03	1.91E+03	5.1	5.14	1
236250262	10.98	6533	4	9	1.0E+03	1.13E+03	18.5	18.56	1
236311085	11.67	6511	2	4	4.6E+02	4.70E+02	20.2	20.18	1
236338125	11.10	6498	9	36	8.1E+02	8.74E+02	16.7	16.63	1
236420722	11.46	8643	5	20	5.3E+02	6.35E+02	7.6	7.63	1
237711874	11.14	7095	7	9	6.0E+02	6.79E+02	17.5	23.31	0

(Continued)

TABLE 3 | Continued

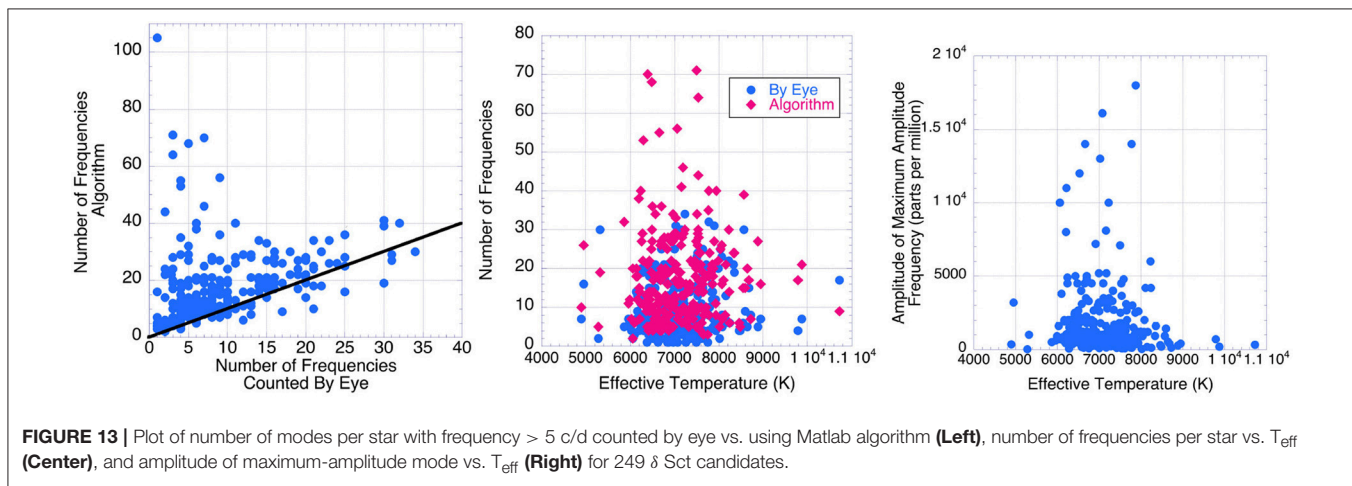
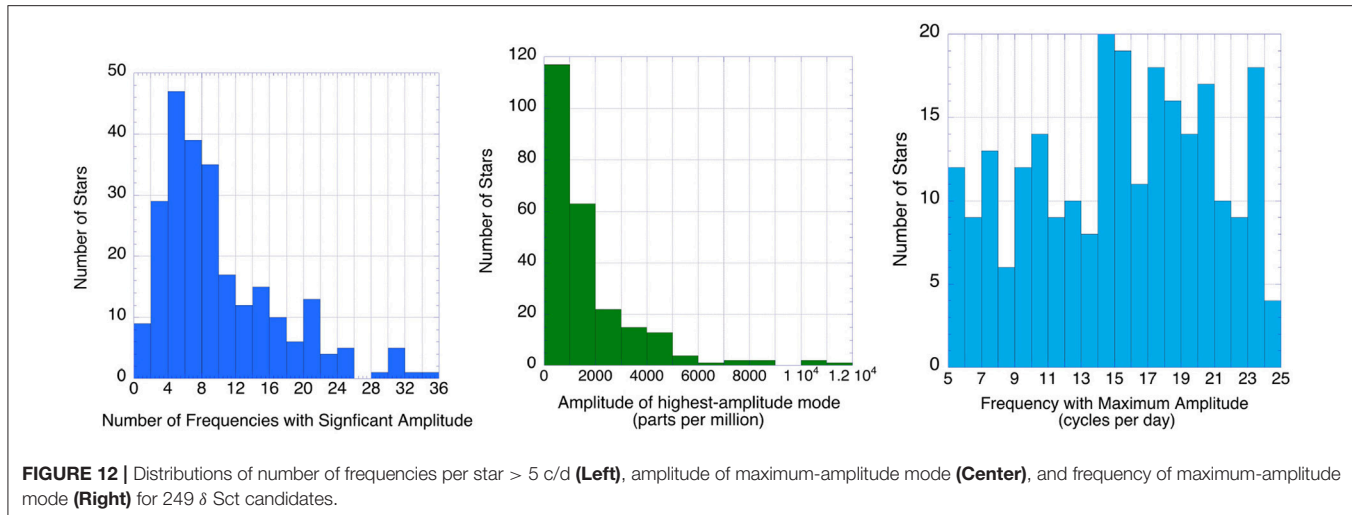
EPIC	Kp mag	T _{eff} (K)	# Freqs.	# Freqs. ^M	A _{max} (ppm)	A _{max} ^M (ppm)	v _{A_{max}} (c/d)	v _{A_{max}} ^M (c/d)	Hybrid flag
237719954	11.44	6656	4	55	4.2E+02	5.14E+02	7.0	6.96	1
237768774	11.64	6988	7	10	3.2E+03	3.43E+03	10.4	9.78	0
237911727	9.48	6474	7	25	4.5E+03	2.92E+03	5.5	7.10	1
237944799	8.83	7094	12	16	8.0E+02	8.33E+02	11.8	11.83	0
237969415	8.39	7857	12	16	7.0E+02	6.95E+02	20.3	20.22	0
237987964	6.31	9785	4	17	7.0E+02	8.49E+02	7.0	7.02	1
240292657	11.09	7224	5	9	1.0E+04	1.02E+04	10.7	10.68	0
240296875	10.79	6680	17	26	3.5E+03	3.89E+03	12.0	12.49	1
240323947	11.51	8548	6	15	6.1E+04	8.18E+04	5.2	5.23	0
240378036	10.82	8140	7	8	1.7E+02	1.74E+02	23.1	23.09	0
240642822	11.08	7790	10	24	3.0E+03	3.66E+03	10.2	10.25	0
240686489	10.48	6566	21	34	4.0E+03	5.55E+03	11.7	9.26	1
242088649	9.24	7345	9	7	1.2E+03	1.70E+03	20.0	20.02	1
242088762	8.82	7345	8	9	8.5E+02	1.16E+03	20.0	20.02	1
242099103	11.37	7426	15	21	1.1E+03	1.15E+03	13.6	13.63	0
242138878	10.98	7660	10	8	2.0E+03	2.15E+03	23.4	23.43	0
242171743	9.78	7421	5	11	9.0E+02	9.01E+02	14.1	14.16	0
245910293	8.53	7494	3	71	8.0E+02	9.08E+02	15.1	15.14	1
245984590	9.85	7154	30	41	1.6E+03	2.58E+03	12.2	12.08	0
246029438	11.47	7934	4	8	2.6E+03	3.42E+03	14.5	14.59	0
246031849	7.53	7644	15	19	3.1E+03	3.43E+03	14.6	14.60	0
246094180	8.28	7072	10	16	3.2E+03	3.31E+03	9.9	9.93	0
246101155	7.83	7555	6	15	6.8E+01	9.75E+01	5.2	5.18	1
246123792	8.15	7775	8	18	1.4E+04	1.39E+04	9.2	9.22	1
246130239	8.67	7489	8	27	1.2E+03	1.74E+03	14.0	13.49	1
246228220	7.61	7816	20	19	1.5E+03	1.57E+03	22.6	17.60	1
246235560	8.96	6660	4	11	1.4E+04	1.29E+04	10.3	10.22	1
246295525	13.63	7584	3	4	4.8E+03	5.11E+03	17.1	17.41	0
246351401	9.10	6763	21	18	9.0E+02	9.96E+02	18.2	18.24	0
246390686	9.76	7652	10	14	2.7E+03	2.68E+03	17.2	17.26	0
246448276	10.19	7015	3	20	7.0E+02	7.73E+02	5.1	6.01	1
246460499	7.54	8072	8	16	1.2E+03	1.12E+03	15.0	14.98	0
246755448	15.05	7094	6	9	4.5E+03	4.62E+03	16.2	16.25	1
246765955	10.81	7556	3	24	1.1E+03	1.02E+03	19.9	19.94	0
246792876	10.51	7931	12	11	4.4E+02	6.67E+02	11.0	10.49	0
246889963	14.34	7457	3	22	1.2E+03	1.35E+03	19.6	19.61	1
246892566	14.46	7092	16	19	8.0E+02	1.27E+03	13.3	13.30	0
246895097	8.60	8944	7	16	4.1E+02	4.20E+02	15.7	15.86	0
246952727	9.03	7764	4	35	6.1E+02	8.38E+02	9.3	9.34	1
246969097	15.15	6803	2	5	4.0E+02	3.77E+02	6.7	6.68	1
247227122	6.17	5863	5	32	5.0E+02	6.63E+02	11.4	11.43	1
247236218	8.41	5279	2	5	2.5E+01	3.11E+01	5.5	5.06	1
247244984	15.36	6433	18	22	1.6E+03	1.67E+03	6.0	5.96	1
247249443	14.49	7217	11	13	1.2E+03	1.29E+03	20.2	20.16	0
247251791	15.81	5987	6	12	9.0E+02	9.43E+02	20.9	20.87	0
247255798	15.80	6648	7	9	2.0E+03	2.14E+03	23.5	23.46	0
247261516	13.61	6616	4	5	6.4E+02	7.77E+02	14.2	14.25	1
247264515	15.89	7495	4	5	3.7E+02	3.65E+02	7.2	7.24	1
247268706	14.48	6649	3	12	4.5E+03	4.75E+03	15.7	15.83	0
247278455	14.29	7944	6	40	1.2E+03	1.23E+03	18.4	18.42	1

(Continued)

TABLE 3 | Continued

EPIC	Kp mag	Teff (K)	# Freqs.	# Freqs. ^M	A _{max} (ppm)	A _{max} ^M (ppm)	v _{A_{max}} (c/d)	v _{A_{max}} ^M (c/d)	Hybrid flag
247292095	15.54	6541	4	7	4.5E+02	4.39E+02	18.8	18.82	0
247295392	15.19	6412	3	4	2.5E+03	2.82E+03	10.8	10.77	0
247319900	15.87	6094	3	6	3.8E+03	3.78E+03	19.5	19.48	1
247321564	10.14	8676	15	17	4.0E+02	5.54E+02	20.0	19.98	1
247333962	15.89	6361	6	10	2.1E+03	2.36E+03	9.0	9.04	1
247338349	15.39	6256	20	27	2.0E+03	2.31E+03	12.4	12.34	1
247382496	15.51	6164	13	12	1.9E+03	2.67E+03	13.3	13.30	0
247382770	15.70	6837	21	25	1.2E+03	1.27E+03	20.8	21.73	0
247383620	13.59	6238	11	40	4.9E+03	5.46E+03	6.8	6.86	1
247465892	15.84	6477	5	14	1.4E+03	1.82E+03	7.8	7.94	1
247473022	15.45	6850	13	16	7.2E+02	8.01E+02	16.0	15.52	1
247473204	15.14	7533	16	30	3.7E+03	4.82E+03	11.6	10.60	0
247481643	14.94	6580	4	6	1.6E+02	2.17E+02	23.2	23.19	0
247504599	14.76	6490	7	10	2.2E+03	2.35E+03	23.2	23.37	0
247505615	14.35	6838	4	8	1.2E+03	1.25E+03	14.8	14.82	1
247511123	15.84	6057	6	20	1.0E+04	9.88E+03	12.4	12.34	0
247526175	14.68	6432	5	9	7.2E+02	9.29E+02	10.7	10.57	1
247544254	15.10	6213	8	14	1.1E+03	1.12E+03	14.8	14.85	1
247553546	15.19	7320	3	5	1.2E+03	1.49E+03	19.2	19.15	0
247576531	15.47	6407	7	11	8.0E+02	8.87E+02	24.1	24.07	0
247584516	7.55	7532	2	44	8.0E+01	1.15E+03	15.7	15.69	1
247598095	13.06	6935	16	28	1.1E+03	1.23E+03	18.4	18.37	1
247606589	15.71	6707	6	6	6.0E+02	7.32E+02	19.1	21.39	0
247608052	14.23	6686	4	17	2.3E+03	2.25E+03	18.0	17.93	0
247648610	9.10	6869	1	4	8.0E+02	1.02E+03	21.5	21.50	0
247650349	15.66	7302	4	7	1.4E+03	1.54E+03	6.6	6.64	1
247676134	13.71	7169	13	28	5.2E+03	5.78E+03	10.6	10.53	0
247698817	12.78	7378	5	10	3.7E+02	4.70E+02	23.7	23.73	0
247700654	15.67	6310	8	11	6.1E+02	8.56E+02	21.2	21.21	0
247702571	9.41	6911	8	27	7.2E+03	8.04E+03	9.4	9.39	1
247708413	15.13	6448	10	12	1.3E+03	1.32E+03	24.2	24.16	0
247708505	13.96	6489	18	30	1.4E+03	1.62E+03	19.6	17.44	0
247714857	14.24	6167	9	18	2.0E+03	2.64E+03	15.3	15.25	0
247743444	15.70	6285	19	22	1.5E+03	1.63E+03	18.2	17.04	0
247749294	15.64	6134	14	18	8.5E+02	1.01E+03	19.7	12.74	0
247760775	14.16	6867	7	12	2.7E+03	2.75E+03	16.7	16.77	1
247764363	7.79	7277	2	14	2.1E+02	2.24E+02	10.1	10.06	1
247766003	15.71	6409	4	5	2.4E+03	2.70E+03	19.0	18.94	1
247768006	15.89	6531	5	9	1.2E+04	1.38E+04	13.9	13.85	0
247770898	15.83	6413	5	13	1.4E+03	1.42E+03	7.3	7.25	0
247811337	15.67	6362	10	9	7.0E+02	7.39E+02	20.2	17.22	1
247828212	15.32	6750	6	7	1.3E+02	1.42E+02	13.9	21.99	1
247841082	15.77	6027	4	7	1.6E+03	1.84E+03	22.3	22.22	0
247877340	15.79	6668	4	4	5.5E+02	7.37E+02	18.1	23.23	1
247899700	14.62	5957	7	11	6.2E+02	6.30E+02	22.6	22.57	0
247917882	6.26	8883	5	27	2.6E+02	2.57E+02	12.2	4.87	1
247931858	15.66	6703	2	4	6.4E+02	5.77E+02	19.7	19.80	0
248122534	15.03	7543	16	17	1.3E+03	1.34E+03	23.0	23.02	0
248125694	15.63	6378	1	5	1.1E+03	1.11E+03	19.0	19.64	0
248186557	14.37	6366	4	13	3.8E+02	4.01E+02	5.6	5.59	1
248264996	11.45	6925	3	10	1.0E+03	1.21E+03	6.4	6.40	1

^a The superscript M refers to the values determined by the Matlab algorithm.



As stated by Bowman and Kurtz (2018), “The full scientific potential of studying δ Sct stars is as yet unrealized.” The δ Sct variables inspire many questions: Why are all of the frequencies expected by linear pulsation theory not observed? Why is it so difficult to find patterns or correlations between stellar properties and pulsation properties such as pulsation amplitudes and frequency content? Some correlations have been discussed in the literature, for example between stellar properties and mean frequency spacings, with the spacings interpreted as a large separation correlated with mean density, or possibly a rotational splitting frequency (see e.g., García Hernández et al., 2015; Paparó et al., 2016a,b; Moya et al., 2017; Bowman and Kurtz, 2018). Why do some stars in the instability regions not show pulsations (see, e.g., Balona, 2013; Murphy et al., 2015)? Why are there so many hybrid γ Dor/ δ Sct variables scattered throughout the pre-*Kepler* theoretical instability regions of both stellar types? What determines the amplitudes of individual modes? Why do amplitudes or frequency content vary with time (Bowman et al., 2017; Breger et al., 2017)?

The *Kepler* and K2 data will be valuable for asteroseismic modeling to address these unsolved problems for A-F type

main-sequence stars. Two questions that these K2 data will help to address are: If the star was known as a δ Sct being identified in the *Kepler* data, has its amplitudes or frequency content changed over time? Can additional frequencies be found using the high signal-to-noise data of *Kepler*/K2? The K2 targets are in general brighter than those in the original *Kepler* field, and are easier to observe using ground- or space-based spectroscopic and photometric observations, or other techniques such as interferometry, to provide long-term monitoring or additional constraints.

AUTHOR CONTRIBUTIONS

JGu was responsible for the design, writing, content, figure, and table creation and selection for this paper. JGu was the author and Principle Investigator for the K2 GO proposals to obtain data used in this paper. JGa wrote the Python interface to plot light curves and amplitude spectra, classify targets, and create **Figures 1–9**. JGu used this interface to examine the data for each K2 target observed and to select the candidate δ Sct stars presented. JGu counted the number

of frequencies and determined the amplitudes and frequency of the maximum-amplitude p mode by eye, and also reviewed each star using SIMBAD for alternate identifiers, descriptors of known variables, and number of references per star. JJ wrote the Matlab algorithm to pre-whiten spectra and count frequencies, search for combination frequencies, and determine amplitudes and frequency of the maximum-amplitude p mode.

FUNDING

JGu's research is supported at Los Alamos National Laboratory (LANL), managed by Triad National Security, LLC for the U.S. Department of Energy's NNSA, Contract #89233218CNA000001. JJ and JGa acknowledge support from NASA under cooperative agreement number NNX17AF74G.

REFERENCES

- Aerts, C., Christensen-Dalsgaard, J., and Kurtz, D. W. (2010). "Astronomy and Astrophysics Library," *Asteroseismology* (Heidelberg: Springer Science+Business Media B.V.).
- Balona, L. A. (2013). "Activity in A-type stars," in *Progress in Physics of the Sun and Stars: A New Era in Helio- and Asteroseismology*, ASP Conference Proceedings, Vol. 479, eds H. Shibahashi, and A. E. Lynas-Gray (San Francisco, CA), 385.
- Balona, L. A. (2018). Gaia luminosities of pulsating A-F stars in the Kepler field. *Month. Not. R. Astron. Soc.* 479, 183–191. doi: 10.1093/mnras/sty1511
- Borucki, W. J., Koch, D., Basri, G., Batalha, N., Brown, T., Caldwell, D., et al. (2010). Kepler planet-detection mission: introduction and first results. *Science* 327, 977–980. doi: 10.1126/science.1185402
- Bowman, D. M., and Kurtz, D. W. (2018). Characterizing the observational properties of δ Sct stars in the era of space photometry from the Kepler mission. *Month. Not. R. Astron. Soc.* 476, 3169–3184. doi: 10.1093/mnras/sty449
- Bowman, D. M., Kurtz, D. W., Breger, M., Murphy, S. J., and Holdsworth, D. L. (2017). Amplitude modulation in δ Sct stars: statistics from an ensemble of Kepler targets. *Eur. Phys. J. Web Conf.* 160:03008. doi: 10.1051/epjconf/201716003008
- Breger, M., Montgomery, M. H., Lenz, P., and Pamyatnykh, A. A. (2017). Nonradial and radial period changes of the δ Scuti star 4 CVn. II. Systematic behavior over 40 years. *Astron. Astrophys.* 599:A116. doi: 10.1051/0004-6361/201629797
- García Hernández, A., Martín-Ruiz, S., Monteiro, M. J. P. F. G., Suárez, J. C., Reese, D. R., Pascual-Granado, J., et al. (2015). Observational $\Delta\nu - \rho$ relation for δ scit stars using eclipsing binaries and space photometry. *Astrophys. J. Lett.* 811:L29. doi: 10.1088/2041-8205/811/2/L29
- Gilliland, R. L., Brown, T. M., Christensen-Dalsgaard, J., Kjeldsen, H., Aerts, C., Appourchaux, T., et al. (2010). Kepler asteroseismology program: introduction and first results. *Public. Astron. Soc. Pac.* 122:131. doi: 10.1086/650399
- Grigahcène, A., Antoci, V., Balona, L., Catanzaro, G., Daszyńska-Daszkiewicz, J., Guzik, J. A., et al. (2010). Hybrid γ doradus- δ scuti pulsators: new insights into the physics of the oscillations from kepler observations. *Astrophys. J. Lett.* 713, L192–L197. doi: 10.1088/2041-8205/713/2/L192
- Heber, U. (2016). Hot subluminous stars. *Public. Astron. Soc. Pac.* 128:082001. doi: 10.1088/1538-3873/128/966/082001
- Howell, S. B., Sobeck, C., Haas, M., Still, M., Barclay, T., Mullally, F., et al. (2014). The K2 mission: characterization and early results. *Public. Astron. Soc. Pac.* 126:398. doi: 10.1086/676406
- Huber, D., Bryson, S. T., and et al. (2017). *VizieR Online Data Catalog: K2 Ecliptic Plane Input Catalog (EPIC)* (Huber+, 2017). Université de Strasbourg/CNRS.
- Huber, D., Bryson, S. T., Haas, M. R., Barclay, T., Barentsen, G., Howell, S. B., et al. (2016). The K2 Ecliptic Plane Input Catalog (EPIC) and stellar classifications of 138,600 targets in campaigns 1-8. *Astrophys. J. Suppl. Ser.* 224:2. doi: 10.3847/0067-0049/224/1/2
- Liakos, A., and Niarchos, P. (2017). Catalogue and properties of δ Scuti stars in binaries. *Month. Not. R. Astron. Soc.* 465, 1181–1200. doi: 10.1093/mnras/stw2756
- Lundkvist, M. S., Huber, D., Silva Aguirre, V., and Chaplin, W. J. (2018). "Using asteroseismology to characterise exoplanet host stars," in *Handbook of Exoplanets*, eds H. J. Deeg and J. A. Belmonte (Basel: Springer Nature), 1655–1678.
- Moya, A., Suárez, J. C., García Hernández, A., and Mendoza, M. A. (2017). Semi-empirical seismic relations of A-F stars from COROT and Kepler legacy data. *Month. Not. R. Astron. Soc.* 471, 2491–2497. doi: 10.1093/mnras/stx1717
- Murphy, S. J., Bedding, T. R., Niemczura, E., Kurtz, D. W., and Smalley, B. (2015). A search for non-pulsating, chemically normal stars in the δ Scuti instability strip using Kepler data. *Month. Not. R. Astron. Soc.* 447, 3948–3959. doi: 10.1093/mnras/stu2749
- Murphy, S. J., Shibahashi, H., and Kurtz, D. W. (2013). Super-Nyquist asteroseismology with the Kepler Space Telescope. *Month. Not. R. Astron. Soc.* 430, 2986–2998. doi: 10.1093/mnras/stt105
- Paparó, M., Benkő, J. M., Hareter, M., and Guzik, J. A. (2016a). Unexpected series of regular frequency spacing of δ scuti stars in the non-asymptotic regime. I. The Methodology. *Astrophys. J.* 822:100. doi: 10.3847/0004-637X/822/2/100
- Paparó, M., Benkő, J. M., Hareter, M., and Guzik, J. A. (2016b). Unexpected series of regular frequency spacing of δ scuti stars in the non-asymptotic regime. II. Sample-echelle diagrams and rotation. *Astrophys. J. Suppl. Ser.* 224:41. doi: 10.3847/0067-0049/224/2/41
- Poretti, E. (2003). Asteroseismology of HADS stars: V974 Oph, a radial pulsator flavoured by nonradial components. *Astron. Astrophys.* 409, 1031–1035. doi: 10.1051/0004-6361:20031223
- Uytterhoeven, K., Moya, A., Grigahcène, A., Guzik, J. A., Gutiérrez-Soto, J., Smalley, B., et al. (2011). The Kepler characterization of the variability among A- and F-type stars. I. General overview. *Astron. Astrophys.* 534:A125. doi: 10.1051/0004-6361/201117368

ACKNOWLEDGMENTS

The authors thank the K2 GO Program for the opportunity to propose targets, and for obtaining outstanding data over many years. The authors also made use of the MAST K2 EPIC target search and data archive, SIMBAD database, and K2 Field-of-View tool as implemented by the *Kepler* Asteroseismic Science Consortium. JGu thanks A. Pigulski for assistance with K2 GO proposals for C4, 5, and 7, observing open clusters. JGu thanks Reiner Friedel of the Center for Earth and Space Science at LANL and Chris Fryer (CCS-2, LANL) for support to attend the NM Astronomy Symposium in November 2018 to present this work, and the New Mexico Consortium for encouragement and assistance in preparing and submitting GO proposals. The authors also thank the reviewers for helpful comments and suggestions.

Conflict of Interest Statement: The authors declare that the research was conducted in the absence of any commercial or financial relationships that could be construed as a potential conflict of interest.

Copyright © 2019 Guzik, Garcia and Jackiewicz. This is an open-access article distributed under the terms of the Creative Commons Attribution License (CC BY). The use, distribution or reproduction in other forums is permitted, provided the original author(s) and the copyright owner(s) are credited and that the original publication in this journal is cited, in accordance with accepted academic practice. No use, distribution or reproduction is permitted which does not comply with these terms.